

---

# An emission line analysis of MASH Galactic Planetary Nebulae

Anna Kovacevic<sup>1</sup> and Quentin Parker<sup>1,2</sup>

<sup>1</sup> Macquarie University [akovac@ics.mq.edu.au](mailto:akovac@ics.mq.edu.au)

<sup>2</sup> Anglo-Australian Observatory [qap@ics.mq.edu.au](mailto:qap@ics.mq.edu.au)

**Summary.** We present preliminary spectrophotometric results for Galactic Planetary Nebulae (PNe) in the Macquarie/AAO/Strasbourg H-alpha Planetary Nebulae Catalogue (MASH) [3]. MASH PNe generally represent the more evolved end of the luminosity function than previous catalogues due to the inherent depth and resolution of the data. Excitation classes are derived for the sample from the available spectroscopy and confirm new trends established by [5]. The excitation classes are compared to other observed PNe properties such as morphology, electron density and Galactic location.

**Key words:** Planetary nebulae, spectroscopy, plasma diagnostics, excitation class.

## 1 Introduction

Emission line ratios in gaseous nebulae provide valuable insight into the internal conditions and physical processes taking place. Plots of various optical line ratios such as  $[\text{OIII}]/\text{H}\beta$ ,  $\text{HeII}/\lambda 4363$ ,  $[\text{NII}]/\text{H}\alpha$  and  $[\text{SII}]/\text{H}\alpha$  can help distinguish between various types of nebulae, especially between supernova remnants, HII regions, Herbig-Haro objects and planetary nebulae.

Results presented here provide a preliminary view into underlying trends of excitation class and electron density against morphology for Galactic PNe. Of the entire MASH-I sample of 904 PNe, only those 325 candidates observed with the 1.9m telescope at the South African Astronomical Observatory (SAAO) between 1999 and 2004 were selected for this study as representing a homogeneous sub-sample in terms of instrumental stability. Measurements of the individual PNe line fluxes for this sample had already been obtained in 2006, so analysis of this data was relatively straightforward. The SAAO PNe used are distributed evenly across the survey region in Galactic latitude and longitude apart from the dense Bulge region, providing an unbiased sub-sample of the non-Bulge MASH sample.

## 2 Excitation class

From this sample of 325 PNe only 197 had the necessary spectral lines with S/N adequate to derive an robust excitation class following the method proposed by [1, 2] as briefly outlined below.

The ratio of the intensities of the  $F(N_1+N_2)/F(4686 \text{ HeII})$  emission lines were initially measured to assign a placement of excitation for those in the medium to high classes. This is however, a highly sensitive indicator so its logarithm is taken and intervals are divided within that scale as shown in Table 1.

Low		Medium		High	
p	$(N_1+N_2)/H\beta$	p	$\log((N_1+N_2)/4686 \text{ HeII})$	p	$\log((N_1+N_2)/4686 \text{ HeII})$
1	0-5	4	>2.6	9	1.7
2	5-10	5	2.5	10	1.5
3	10-15	6	2.3	11	1.2
4	>15	7	2.1	12	0.9
		8	1.9	12+	0.6

**Table 1.** Depending on the above values, PNe will be grouped into either the low (p=1-4), medium (p=5-8) or high (p=9-12+) excitation class.

In this scheme, objects are immediately grouped into the medium and high classes based on the definite presence of the 4686 HeII emission line. Each excitation class 'p', based on the magnitude of the ratio  $\log F(N_1+N_2)/F(4686)$  corresponds to the limits  $\pm 0.1$ . Members in the 12+ excitation class are very high excitation with nuclei temperatures equivalent to 300,000 K and above. For those objects whose spectra exhibit very weak (ie barely distinguishable from the noise) or no 4686 HeII, they are classified into the low excitation classes p = 1-4 based on the observed ratio of intensities of the  $F(N_1+N_2)/F(H\beta)$  emission lines. The excitation classes 4 and 12+ are unique in that they have open limits. PNe whose magnitudes of  $\log F(N_1+N_2)/F(4686) < 0.6$  are classified into the 12+ class and those whose spectra lacks evidence of any definite 4686 HeII but have  $F(N_1+N_2)/F(H\beta) > 20$  are grouped into excitation class 4. Typically, low excitation spectra have a high [NII]/H $\alpha$  ratio and little or no HeII 4686 present, whereas high excitation spectra often have strong H $\alpha$ , no [NII] and strong 4686 HeII.

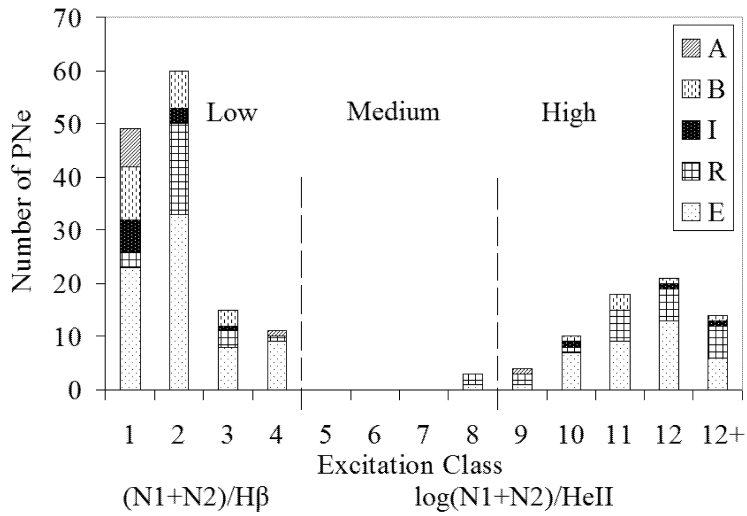
Our data were obtained with a low-resolution grating angled to cover the main optical spectrum from 3700-7500Å. The CCD is less efficient in the blue and the region is more susceptible to the effects of Galactic extinction so emission lines here were typically of lower S/N (and therefore subject to greater error) than lines in the red. Hence, this system is preferred to that proposed by [4] as although their method would eliminate any effects abundances may have on excitation class, by using lines originating from different elements, the emission lines they use are generally weaker than those used by [1, 2] and not available for most PNe.

Of the spectra presented here, 19 had repeat SAAO observations, often done for data integrity/repeatable checks, or occasionally because the first observation was of poorer quality. Line fluxes were re-measured for this repeat sample. Despite the modest S/N differences, the spectra for 13 of these repeat objects yielded excitation

classes in complete agreement while 4 objects' excitation classes differed by only 1 between each spectra. There were, however, 2 cases where the excitation class differed by 2 but these were for objects with high S/N difference between repeats. The chosen excitation class for these final 6 objects was based the highest S/N spectra.

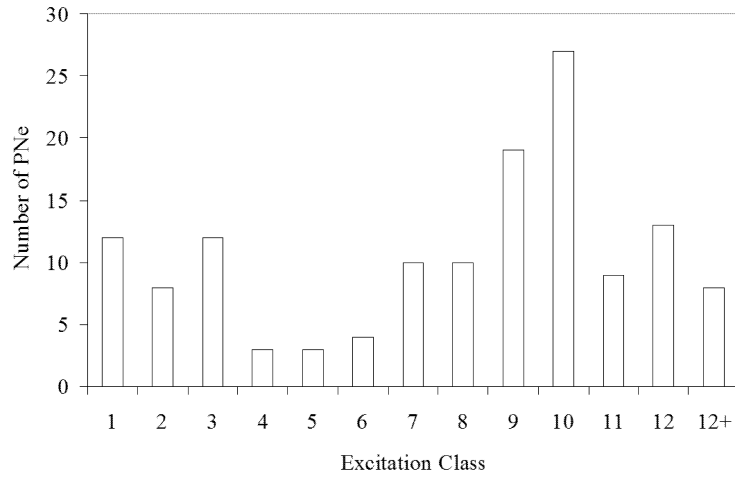
### 3 Results

Figure 1 displays the representative sample of SAAO observed MASH PNe distributed into their corresponding excitation classes. For comparison, figure 2 displays the excitation class distribution for 138 previously known Galactic PNe listed in [2].



**Fig. 1.** MASH excitation class results from the SAAO sample. The patterns within the bars represent the different morphologies.

The most important result here is that MASH has not uncovered many additional medium excitation PNe and that the numbers of high and low excitation PNe are substantially increased. Interestingly, this result is exactly the same as found for a new sample of  $\sim 470$  PNe in the Large Magellanic Cloud (LMC) uncovered by [5]. Most known Galactic PNe have higher surface brightness due to past surveys being limited in depth and having bright [OIII] lines due to survey selection, so both the MASH and LMC samples, selected in  $H\alpha$  imaging, are populations complete to fainter magnitudes and cover a wider evolutionary range. By comparing figures 1 & 2 it can be seen that these lower surface brightness objects typically populate the more extreme excitation classes.



**Fig. 2.** Excitation class distribution of 138 Galactic PNe as listed in [2].

The bars representing the number of MASH PNe in each excitation class in figure 1 are fractionally split into various patterns representing the different morphological types occupying those excitation classes. There is a trend observed with bipolars, asymmetricals and irregular PNe tending to be of lower excitation class.

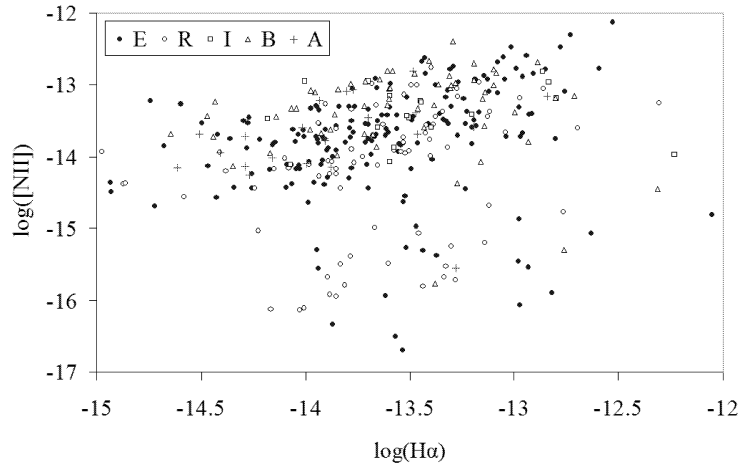


**Fig. 3.** The distribution of the morphology of PNe are presented as a function of their [NII] and  $H\alpha$  fluxes measured in  $\text{ergs m}^{-2} \text{s}^{-1}$ . There are two trends apparent here.

Figure 3 looks more explicitly at the distribution of morphological class with  $[\text{NII}]/\text{H}\alpha$ . As well as there being a definite correlation between morphology and  $[\text{NII}]$  flux, there is also the suggestion that, for ellipticals and round PNe at least, there may be two trend lines present: a main broad linear correlation populated mainly by the bipolars, asymmetricals and irregulars, and a second trend of higher excitation running in parallel just below it, primarily containing round and elliptical PNe.

In order to suppress any possible scatter by objects of large angular diameter due to varying excitation across their area, a distribution of the objects' diameter as a function of  $[\text{NII}]$  vs.  $\text{H}\alpha$  was also constructed. No correlation between the average diameter of the PNe and outlying data points was found.

Electron densities were also derived for 148 objects out of the 325 for which  $[\text{SII}]$  lines were definitely present at the satisfactory S/N. The electron density was calculated by taking the ratio between the  $\lambda 6717/\lambda 6731$   $[\text{SII}]$  lines. The electron density of all PNe were then plotted to see if there was any trend evident between their morphology and electron density. No obvious correlation in angular diameter or morphology with respect to electron densities was found.

## References

1. G.A. Gurzadyan: *Ap&SS* **149** 343 (1988)
2. G.A. Gurzadyan., A.G. Egikyan: *Ap&SS* **181** 73 (1991)
3. Q. Parker et. al: *MNRAS* **373** 79 (2006)
4. M.A. Ratag, S.R. Pottasch, M. Dennefeld, J. Menzies: *A&AS* **126** 297 (1997)
5. W. Reid, Q.A. Parker: *MNRAS* **365** 401 (2006)